Available online at www.sciencedirect.com
ScienceDirect
Journal of Sound and Vibration 318 (2008) 884–902
JOURNAL OF SOUND AND VIBRATION
www.elsevier.com/locate/jsvi

Modelling wave propagation in two-dimensional structures using finite element analysis

Brian R. Mace[a,*], Elisabetta Manconi[b]

[a]*Institute of Sound and Vibration Research, University of Southampton, Highfield, Southampton SO17 1BJ, UK*
[b]*Department of Industrial Engineering, University of Parma, Parco Area delle Scienze 181/A, 43100 Parma, Italy*

Received 26 January 2008; accepted 21 April 2008
Handling Editor: C.L. Morfey
Available online 6 June 2008

Abstract

A method is described by which the dispersion relations for a two-dimensional structural component can be predicted from a finite element (FE) model. The structure is homogeneous in two dimensions but the properties might vary through the thickness. This wave/finite element (WFE) method involves post-processing the mass and stiffness matrices, found using conventional FE methods, of a segment of the structure. This is typically a 4-noded, rectangular segment, although other elements can be used. Periodicity conditions are applied to relate the nodal degrees of freedom and forces. The wavenumbers—real, imaginary or complex—and the frequencies then follow from various resulting eigenproblems. The form of the eigenproblem depends on the nature of the solution sought and may be a linear, quadratic, polynomial or transcendental eigenproblem. Numerical issues are discussed. Examples of a thin plate, an asymmetric laminated plate and a laminated foam-cored sandwich panel are presented. For the last two examples, developing an analytical model is a formidable task at best. The method is seen to give accurate predictions at very little computational cost. Furthermore, since the element matrices are typically found using a commercial FE package, the meshing capabilities and the wealth of existing element libraries can be exploited.

1. Introduction

The propagation of waves in a homogeneous structure is of interest for many applications, especially at higher frequencies. Examples include the transmission of structure-borne sound, shock response and statistical energy analysis. Knowledge of the dispersion relations, group velocity, reflection and transmission characteristics, etc., enables predictions to be made of disturbance propagation, energy transport and so on.

In simple cases, analytical expressions for the dispersion equation can be found (e.g. Refs. [1,2]). Examples include one-dimensional structures such as rods and thin beams and two-dimensional structures such as thin plates. For more complicated structures or at higher frequencies the analysis becomes more difficult or even impossible, and the dispersion equation is usually transcendental. Finding all the real, imaginary and complex

*Corresponding author. Tel.: +44 23 8059 3605; fax: +44 23 8059 3190.
E-mail addresses: brm@isvr.soton.ac.uk (B.R. Mace), elisabetta.manconi@unipr.it (E. Manconi).

0022-460X/$ - see front matter © 2008 Elsevier Ltd. All rights reserved.
doi:10.1016/j.jsv.2008.04.039

solutions can be difficult and numerical solutions might be sought. Perhaps the underlying assumptions and approximations break down—for example, for a plate, Kirchoff [1,2], Mindlin [1–3] or Rayleigh-Lamb [1,4] theories might be required to accurately model the behaviour as frequency increases. On the other hand, the properties of the cross-section of a homogeneous solid might be complicated. Examples include layered media and laminated, fibre-reinforced, composite constructions. The latter might be modelled as single equivalent uniform plates but at higher frequencies first (or higher-order) shear deformation theories [5,6] might be necessary. The equations of motion then become very complicated at best.

Thus in such cases numerical approaches are potentially of benefit. In this paper a finite element (FE)-based approach for the analysis of wave propagation in homogeneous, two-dimensional structures is described. The properties can vary in an arbitrary manner through the thickness of the structure. In this wave/finite element (WFE) method the mass and stiffness matrices of a conventional FE model of a very small segment (typically rectangular) of the structure are post-processed by applying periodicity conditions for the propagation of a time-harmonic disturbance through the structure. The approach is similar to that of Abdel-Rahman [7] for the FE analysis (FEA) of periodic structures, except that in the present case the spatial periodicity is arbitrary. Application of the periodicity conditions results in various eigenproblems whose solutions yield the dispersion relations. Since conventional FEA is used, the full power of existing FE packages and their extensive element libraries can be utilised.

For one-dimensional structures there have been applications of the WFE method for free [8] and forced vibration [9], to rail structures [10] (and, in Ref. [11], using periodic structure theory for a track section), laminate plates [8], thin-walled structures [12] and fluid-filled [13,14] pipes. Mencik and Ichchou [15] applied the method to calculate wave transmission through a joint. There have been various applications of FEA to spatially periodic one-dimensional structures. These include the earlier works of Orris and Petyt [16,17], Abdel-Rahman [7] and others reviewed by Mead in Ref. [18]. Specific applications include railway tracks [11], truss beams [19] and stiffened cylinders [20,21]. The general approach is in contrast to the spectral finite element (SFE) method for one-dimensional waveguides (e.g. Refs. [22–24]) in which new elements, with a space-harmonic displacement along the axis of the waveguide, must be derived on a case-by-case basis. Other authors have applied periodic structure theory and FE to two-dimensional structures, for example Ruzzene et al. [25], who considered cellular cored structures. Duhamel [26] presents a similar approach for forced vibration of a two-dimensional structure. In Ref. [26], he enforces a harmonic motion of the form $\exp(-iky)$ in one direction, so that the equation of motion reduces to that for a one-dimensional structure and is subsequently solved using the WFE methods in Refs. [8,9]. The Green function is then found by evaluating an integral over the wavenumber k. This is a similar approach to "two-dimensional" spectral element methods (e.g. Ref. [27]), where a harmonic dependence in one dimension is imposed, so that a two-dimensional structure reduces to an ensemble of one-dimensional waveguides.

This paper extends the WFE approach to two-dimensional homogeneous structures. In Section 2 the formulation is described. Periodic structure theory is employed, although the periodicity is arbitrary. A single segment of the structure is analysed using conventional FE methods. This is typically a rectangular segment, meshed through the structure's thickness with rectangular elements with only corner nodes. Elements with other shapes or with interior or mid-side nodes can also be used. Periodicity conditions are applied to develop eigenproblems of various forms—linear, polynomial or transcendental—whose solutions yield the dispersion relations, group velocity and so on. The eigenvalue problems and various numerical issues are discussed in Section 3. Section 4 contains numerical examples of thin isotropic and orthotropic plates, for which analytical solutions are available, and laminated composite-reinforced plates for which an analytical solution is not available. Further details and examples can be found in Ref. [28].

2. The wave/finite element formulation

Consider a solid which is homogeneous in both the x and y directions, but whose properties may vary through its thickness in the z-direction. An example is the laminate shown in Fig. 1(a), in which each layer is uniform. Under the passage of a time-harmonic wave of frequency ω any response variable $w(x, y, z, t)$

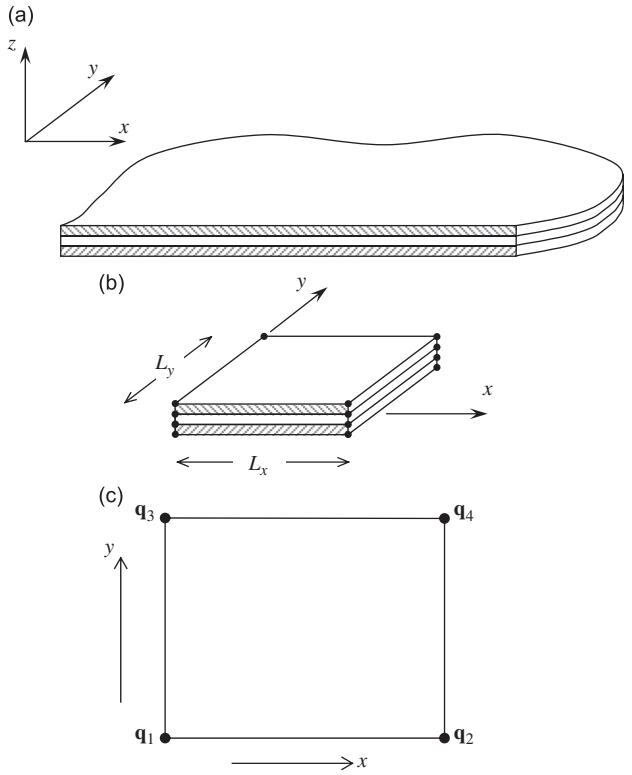

Fig. 1. (a) Two dimensional homogeneous solid, (b) rectangular segment and (c) definition of nodes.

varies as

$$w(x,y,z,t) = W(z)\mathrm{e}^{\mathrm{i}(\omega t - k_x x - k_y y)} \tag{1}$$

where $k_x = k\cos\theta$ and $k_y = k\sin\theta$ are the components of the wavenumber k in the x and y directions and where $W(z)$ is some function through the thickness of the solid that describes the wave mode in terms of the response variable w. The wavenumbers might be real (for propagating waves in the absence of damping), pure imaginary (for evanescent waves) or complex (for oscillating, decaying waves). The propagating waves travel in a direction which is at an angle θ to the x-axis.

The aim is to estimate the dispersion relations between k_x, k_y and ω, together with the variation of displacements, internal forces, stresses and so on through the thickness. Analytical methods are straightforward for simple structures such as thin plates [1,2], but become complicated for more complex structures such as solids whose thickness is comparable to the wavelength [1–4] or laminates where higher-order shear deformation theories might be required [5,6]. In the WFE approach a numerical solution is sought from conventional FEA [29].

A small segment of the structure is taken as shown in Fig. 1(b). The segment is rectangular in the (x,y) plane with sides of lengths L_x and L_y and is meshed through the thickness using 4-noded rectangular finite elements. Such elements are common in FEA. The use of other elements is straightforward and is discussed in Section 2.2. The vector of degrees of freedom (dofs) $\mathbf{q}$ of the segment shown in Fig. 1(c) are given in terms of the nodal dofs by

$$\mathbf{q} = \begin{bmatrix} \mathbf{q}_1^{\mathrm{T}} & \mathbf{q}_2^{\mathrm{T}} & \mathbf{q}_3^{\mathrm{T}} & \mathbf{q}_4^{\mathrm{T}} \end{bmatrix}^{\mathrm{T}} \tag{2}$$

where the superscript T denotes the transpose and where $\mathbf{q}_j$ is the vector of the nodal dofs of all the elements nodes which lie on the jth corner of the element. (Strictly, perhaps, this should be referred to as a hypernode formed by concatenating all the element nodes through the thickness of the segment, although for simplicity it

is referred to subsequently as node j.) Similarly, the vector of nodal forces is

$$\mathbf{f} = \begin{bmatrix} \mathbf{f}_1^{\mathrm{T}} & \mathbf{f}_2^{\mathrm{T}} & \mathbf{f}_3^{\mathrm{T}} & \mathbf{f}_4^{\mathrm{T}} \end{bmatrix}^{\mathrm{T}} \tag{3}$$

The mass and stiffness matrices $\mathbf{M}$ and $\mathbf{K}$ of the segment are found using conventional FE methods. Typically a commercial package might be used so that existing element libraries can be exploited. The equation of motion of the segment, assuming time-harmonic behaviour and neglecting damping, is

$$\left[\mathbf{K} - \omega^2 \mathbf{M}\right]\mathbf{q} = \mathbf{f} \tag{4}$$

Now consider waves propagating through the continuum of Fig. 1(a). The solid is assumed to be modelled, using FEA, as a two-dimensional array of identical rectangular segments as shown in Fig. 1(b). Under the propagation of a wave as in Eq. (1), the nodal dofs are such that

$$\mathbf{q}_2 = \lambda_x \mathbf{q}_1, \quad \mathbf{q}_3 = \lambda_y \mathbf{q}_1, \quad \mathbf{q}_4 = \lambda_x \lambda_y \mathbf{q}_1 \tag{5}$$

where

$$\lambda_x = \mathrm{e}^{-\mathrm{i}\mu_x}, \quad \lambda_y = \mathrm{e}^{-\mathrm{i}\mu_y}, \quad \mu_x = k_x L_x, \quad \mu_y = k_y L_y \tag{6}$$

Here μ_x and μ_y are the propagation constants. Thus

$$\mathbf{q} = \mathbf{\Lambda}_R \mathbf{q}_1, \quad \mathbf{\Lambda}_R = \begin{Bmatrix} \mathbf{I} \\ \lambda_x \mathbf{I} \\ \lambda_y \mathbf{I} \\ \lambda_x \lambda_y \mathbf{I} \end{Bmatrix} \tag{7}$$

In the absence of external excitation, equilibrium at node 1 implies that the sum of the nodal forces of all the elements connected to node 1 is zero. Consequently

$$\mathbf{\Lambda}_L \begin{Bmatrix} \mathbf{f}_1 \\ \mathbf{f}_2 \\ \mathbf{f}_3 \\ \mathbf{f}_4 \end{Bmatrix} = \mathbf{0}, \quad \mathbf{\Lambda}_L = \begin{bmatrix} \mathbf{I} & \lambda_x^{-1}\mathbf{I} & \lambda_y^{-1}\mathbf{I} & \lambda_x^{-1}\lambda_y^{-1}\mathbf{I} \end{bmatrix} \tag{8}$$

Substituting Eq. (7) into Eq. (4) and premultiplying by $\mathbf{\Lambda}_L$ gives

$$\left[\overline{\mathbf{K}}(\lambda_x, \lambda_y) - \omega^2 \overline{\mathbf{M}}(\lambda_x, \lambda_y)\right]\mathbf{q}_1 = \mathbf{0} \tag{9}$$

where

$$\overline{\mathbf{K}} = \mathbf{\Lambda}_L \mathbf{K} \mathbf{\Lambda}_R, \quad \overline{\mathbf{M}} = \mathbf{\Lambda}_L \mathbf{M} \mathbf{\Lambda}_R \tag{10}$$

are the reduced stiffness and mass matrices, i.e. the segment matrices projected onto the dofs of node 1 under the assumption of disturbance propagation as in Eq. (1). The eigenvalue problem of Eq. (9) can also be written as

$$\overline{\mathbf{D}}(\omega; \lambda_x, \lambda_y)\mathbf{q}_1 = \mathbf{0} \tag{11}$$

where $\overline{\mathbf{D}} = \overline{\mathbf{K}} - \omega^2 \overline{\mathbf{M}}$ is the reduced dynamic stiffness matrix (DSM). If the segment DSM is partitioned as

$$\mathbf{D} = \begin{bmatrix} \mathbf{D}_{11} & \mathbf{D}_{12} & \mathbf{D}_{13} & \mathbf{D}_{14} \\ \mathbf{D}_{21} & \mathbf{D}_{22} & \mathbf{D}_{23} & \mathbf{D}_{24} \\ \mathbf{D}_{31} & \mathbf{D}_{32} & \mathbf{D}_{33} & \mathbf{D}_{34} \\ \mathbf{D}_{41} & \mathbf{D}_{42} & \mathbf{D}_{43} & \mathbf{D}_{44} \end{bmatrix} \tag{12}$$

then the eigenproblem (11) becomes

$$[(\mathbf{D}_{11}+\mathbf{D}_{22}+\mathbf{D}_{33}+\mathbf{D}_{44})+(\mathbf{D}_{12}+\mathbf{D}_{34})\lambda_x+(\mathbf{D}_{21}+\mathbf{D}_{43})\lambda_x^{-1} + (\mathbf{D}_{13}+\mathbf{D}_{24})\lambda_y+(\mathbf{D}_{31}+\mathbf{D}_{42})\lambda_y^{-1}+\mathbf{D}_{14}\lambda_x\lambda_y+\mathbf{D}_{41}\lambda_x^{-1}\lambda_y^{-1} + \mathbf{D}_{32}\lambda_x\lambda_y^{-1}+\mathbf{D}_{23}\lambda_x^{-1}\lambda_y]\mathbf{q}_1=0 \tag{13}$$

If there are n dofs per node, the nodal displacement and force vectors $\mathbf{q}_j$ and $\mathbf{f}_j$ are $n\times 1$, the segment mass and stiffness matrices are $4n\times 4n$ while the reduced matrices are $n\times n$. Eqs. (9) and (11) give eigenproblems relating λ_x, λ_y and ω for the discretised structure, whose solutions give FE estimates of the dispersion relations for the continuous structure.

2.1. Damping

The presence of viscous or structural damping can be included by the addition of viscous or structural damping matrices $\mathbf{C}$ or $\mathbf{K}'$. The dynamic stiffness matrix of the segment is now complex and becomes

$$\mathbf{D}=\mathbf{K}+\mathrm{i}\omega\mathbf{C}-\omega^2\mathbf{M}, \quad \text{and} \quad \mathbf{D}=\mathbf{K}+\mathrm{i}\mathbf{K}'-\omega^2\mathbf{M}, \tag{14}$$

respectively.

2.2. Other FE implementations

The method can be applied to cases other than 4-noded, rectangular elements straightforwardly, so that the full power of typical element libraries can be exploited.

2.2.1. Mid-side nodes

Mid-side nodes can be accommodated along the lines described by Abdel-Rahman [7] for periodic structures. Consider the rectangular segment with mid-side nodes shown in Fig. 2(a). Defining the nodal dofs as

$$\mathbf{q}=\begin{bmatrix}\mathbf{q}_1^{\mathrm{T}} & \mathbf{q}_2^{\mathrm{T}} & \mathbf{q}_3^{\mathrm{T}} & \mathbf{q}_4^{\mathrm{T}} & \mathbf{q}_L^{\mathrm{T}} & \mathbf{q}_R^{\mathrm{T}} & \mathbf{q}_B^{\mathrm{T}} & \mathbf{q}_T^{\mathrm{T}}\end{bmatrix}^{\mathrm{T}} \tag{15}$$

the periodicity conditions become

$$\mathbf{q}=\mathbf{\Lambda}_R\begin{Bmatrix}\mathbf{q}_1\\ \mathbf{q}_L\\ \mathbf{q}_B\end{Bmatrix}; \quad \mathbf{\Lambda}_R=\begin{bmatrix}\mathbf{I} & \lambda_x\mathbf{I} & \lambda_y\mathbf{I} & \lambda_x\lambda_y\mathbf{I} & \mathbf{0} & \mathbf{0} & \mathbf{0} & \mathbf{0}\\ \mathbf{0} & \mathbf{0} & \mathbf{0} & \mathbf{0} & \mathbf{I} & \lambda_x\mathbf{I} & \mathbf{0} & \mathbf{0}\\ \mathbf{0} & \mathbf{0} & \mathbf{0} & \mathbf{0} & \mathbf{0} & \mathbf{0} & \mathbf{I} & \lambda_y\mathbf{I}\end{bmatrix}^{\mathrm{T}} \tag{16}$$

Equilibrium at node 1 gives Eq. (8) while equilibrium at the left and bottom mid-side nodes leads to

$$\mathbf{f}_L+\lambda_x^{-1}\mathbf{f}_R=0, \quad \mathbf{f}_B+\lambda_y^{-1}\mathbf{f}_T=0 \tag{17}$$

and hence

$$\mathbf{\Lambda}_L\begin{Bmatrix}\mathbf{f}_1\\ \mathbf{f}_L\\ \mathbf{f}_B\end{Bmatrix}=\begin{Bmatrix}\mathbf{0}\\ \mathbf{0}\\ \mathbf{0}\end{Bmatrix}, \quad \mathbf{\Lambda}_L=\begin{bmatrix}\mathbf{I} & \lambda_x^{-1}\mathbf{I} & \lambda_y^{-1}\mathbf{I} & \lambda_x^{-1}\lambda_y^{-1}\mathbf{I} & \mathbf{0} & \mathbf{0} & \mathbf{0} & \mathbf{0}\\ \mathbf{0} & \mathbf{0} & \mathbf{0} & \mathbf{0} & \mathbf{I} & \lambda_x^{-1}\mathbf{I} & \mathbf{0} & \mathbf{0}\\ \mathbf{0} & \mathbf{0} & \mathbf{0} & \mathbf{0} & \mathbf{0} & \mathbf{0} & \mathbf{I} & \lambda_y^{-1}\mathbf{I}\end{bmatrix} \tag{18}$$

The matrices are again reduced as given by Eq. (10).

In Ref. [28] an approximation which reduces the size of the resulting eigenproblem is suggested by enforcing further periodicity conditions between nodes 1, L and B. In this it is assumed that $\mathbf{q}_L=\lambda_y^{1/2}\mathbf{q}_1, \mathbf{q}_B=\lambda_x^{1/2}\mathbf{q}_1$ so

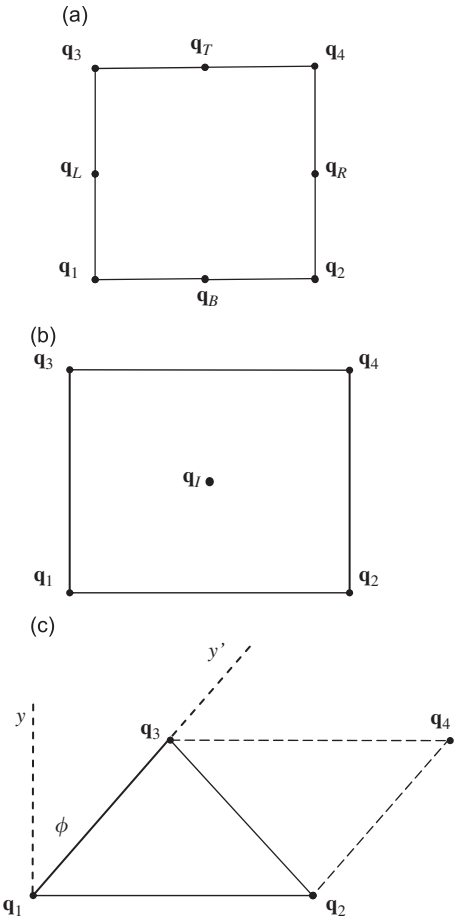

Fig. 2. Other finite element implementations: (a) element with mid-side nodes; (b) element with internal dofs; and (c) triangular element.

that the segment matrices are projected onto the dofs of node 1 only. This introduces some errors which seem to be small in most, if not all, cases of interest.

2.2.2. Internal nodes

Suppose there are internal dofs defined at some internal node I as shown in Fig. 2(b). The dofs can be partitioned into boundary and internal dofs such that

$$\mathbf{D}\begin{Bmatrix}\mathbf{q}\\ \mathbf{q}_I\end{Bmatrix} = \begin{Bmatrix}\mathbf{f}\\ \mathbf{0}\end{Bmatrix} \tag{19}$$

where it is noted that the nodal forces on the internal dofs are zero. The internal dofs can then be removed by dynamic condensation [29].

2.2.3. Triangular elements

Consider the triangular segment with 3 nodes as shown in Fig. 2(c). A second, identical segment is appended so that together they form a parallelogram with one side parallel to the x-axis and another parallel to the direction y' at an angle ϕ to the y-axis. The periodicity conditions and transformation are the same except that now

$$\mathbf{q}_3 = \lambda_{y'}\mathbf{q}_1, \quad \lambda_{y'} = \lambda_y\lambda_x^{(L_y \tan\,\phi/L_x)} \tag{20}$$

3. Forms of the eigenproblem

The eigenproblems of Eqs. (9) and (11) involve the three parameters λ_x, λ_y and ω, and take various forms depending on the physical nature of the solution being sought. As will be seen later, some eigensolutions are artifacts of the spatial discretisation of the structure and are not representative of wave motion in the continuum.

First, the matrices $\mathbf{K}$ and $\mathbf{M}$, and $\mathbf{C}$ and $\mathbf{K}'$ if damping is present, are real and symmetric in the absence of gyroscopic terms. Consequently so, too, is the DSM $\mathbf{D}$. By taking the transpose of Eq. (13) it follows that, for real ω, if (λ_x, λ_y) is a solution to Eq. (13) then so too is any combination of $(\lambda_x, 1/\lambda_x)$ and $(\lambda_y, 1/\lambda_y)$. These four solutions represent the same disturbance travelling in the four directions $\pm\theta$, $\pi\pm\theta$.

3.1. Free wave propagation in undamped structures: linear algebraic eigenvalue problem

To calculate the dispersion relations for free wave propagation in an undamped structure, the propagation constants μ_x and μ_y are given and the corresponding frequencies of free wave propagation are to be found. Eq. (9) then becomes a standard, linear, algebraic eigenvalue problem in ω^2 to which there are thus n solutions. In the undamped case μ_x and μ_y are real and hence $|\lambda_x| = |\lambda_y| = 1$, representing waves that propagate through the structure with a wavenumber $k = \sqrt{k_x^2 + k_y^2}$ and in a direction $\theta = \tan^{-1} k_y/k_x$.

By considering the transpose-conjugate of Eq. (13) it can be shown [28,30] that the reduced stiffness and mass matrices in Eq. (10) are positive definite Hermitian matrices. Therefore, for real μ_x and μ_y, the n eigenvalues ω^2 for which free wave propagation is possible are real and positive. The eigenvectors define the wave modes. Although there are n solutions, not all represent wave motion in the continuous structure, some being artifacts of the spatial discretisation and periodicity as discussed in Section 3.2.

If the structure is damped then real values for μ_x and μ_y imply complex, decaying solutions for ω^2 or, alternatively, for real ω^2 the solutions for μ_x and μ_y are complex and the methods described in the following two subsections must be used.

3.1.1. Group velocity

The group velocity

$$\mathbf{c}_g = \frac{\mathrm{d}\omega}{\mathrm{d}\mathbf{k}} = \frac{\partial \omega}{\partial k_x}\mathbf{i} + \frac{\partial \omega}{\partial k_y}\mathbf{j} \tag{21}$$

where $\mathbf{i}$ and $\mathbf{j}$ are unit vectors in the x and y directions, respectively. The group velocity is in the direction of the normal to the curves in the (k_x, k_y) for constant ω [31]. The derivatives can be found from the eigenvalue problem of Eq. (9) since, for a given eigenvalue ω_j^2 with mass-normalised left and right eigenvectors $\boldsymbol{\psi}_j$ and $\boldsymbol{\phi}_j$ [32]

$$\frac{\partial \omega_j^2}{\partial k_x} = \boldsymbol{\psi}_j \left[\frac{\partial \overline{\mathbf{K}}}{\partial k_x} - \omega_j^2 \frac{\partial \overline{\mathbf{M}}}{\partial k_x} \right] \boldsymbol{\phi}_j \tag{22}$$

with a similar expression for $\partial \omega_j^2/\partial k_y$. In practice the derivatives in Eq. (21) might be estimated numerically using a finite difference approach, as suggested in Ref. [12] for 1-dimensional waveguides. Using a central difference approximation this involves evaluating $\omega(k_x \pm \Delta k_x/2, k_y)$, for example.

3.2. Frequency and one wavenumber known: quadratic eigenvalue problem

In the second class of eigenproblem the frequency ω and one wavenumber, say k_x, are given. This might physically represent the situation where a known wave is incident on a straight boundary so that the (typically real) trace wavenumber along the boundary is given and all possibly solutions for k_y are sought, real, imaginary or complex. Wave propagation in a closed cylindrical shell is a second example, where the wavenumber around the circumference can only take certain discrete values. In this case, Eq. (13) becomes a quadratic in λ_y and a quadratic eigenproblem results, for which there are $2n$ solutions.

3.3. Frequency and direction of wave propagation known: polynomial and transcendental eigenvalue problems

In the third type of eigenproblem the frequency ω and the direction of propagation θ are specified. Hence λ_x and λ_y are of the form

$$\lambda_x = \mathrm{e}^{-\mathrm{i}\mu_x}, \quad \lambda_y = \mathrm{e}^{-\mathrm{i}\mu_y}, \quad \frac{\mu_y}{\mu_x} = \frac{L_y}{L_x}\tan\,\theta \tag{23}$$

where μ_x and μ_y might be complex, but their ratio is real and given. The nature of the eigenproblem depends on whether this ratio is rational or irrational.

3.3.1. Ratio of propagation constants rational: polynomial eigenvalue problem

If the ratio $\mu_y/\mu_x = m_2/m_1$ is rational, m_1 and m_2 being integers with no common divisor, the propagation constants can be written as $\mu_x = m_1\sigma$, $\mu_y = m_2\sigma$. Putting $\gamma = \mathrm{e}^{-\mathrm{i}\sigma}$, the eigenvalue problem (13) can be written in the form

$$\begin{aligned}&\left[\mathbf{A}_0 + \mathbf{A}_1\gamma^{m_1} + \mathbf{A}_2\gamma^{m_2} + \mathbf{A}_3\gamma^{2m_1} + \mathbf{A}_4\gamma^{2m_2} + \mathbf{A}_5\gamma^{m_1+m_2}\right.\\ &\left.+\mathbf{A}_6\gamma^{2m_1+m_2} + \mathbf{A}_7\gamma^{m_1+2m_2} + \mathbf{A}_8\gamma^{2m_1+2m_2}\right]\mathbf{q}_1 = 0\end{aligned} \tag{24}$$

The matrices $\mathbf{A}$ are of order $n \times n$ so that Eq. (24) is a polynomial eigenvalue problem of order $2(m_1+m_2)$ which has $2n(m_1+m_2)$ solutions for γ. The problem can be recast as the standard linear eigenvalue problem

$$(\mathbf{Q} - \gamma\mathbf{I})\mathbf{Z} = \mathbf{0} \tag{25}$$

where

$$\mathbf{Q} = \begin{bmatrix} -\mathbf{A}_m^{-1}\mathbf{A}_{m-1} & \cdots & -\mathbf{A}_m^{-1}\mathbf{A}_1 & -\mathbf{A}_m^{-1}\mathbf{A}_0 \\ \mathbf{I} & \cdots & \mathbf{0} & \mathbf{0} \\ \vdots & \ddots & \vdots & \vdots \\ \mathbf{0} & \cdots & \mathbf{I} & \mathbf{0} \end{bmatrix}, \quad \mathbf{Z} = \begin{Bmatrix} \gamma^{m-1}\mathbf{q} \\ \vdots \\ \gamma\mathbf{q} \\ \mathbf{q} \end{Bmatrix} \tag{26}$$

Clearly the order of the eigenvalue problem might be very large and hence there be very many solutions, only some of which represent free wave propagation in the continuous structure, the rest being solutions relevant only to the discretised problem. In principle this is not an issue since all but a few solutions lie far enough from the origin in the complex kL plane that the finite element discretisation is known to be inaccurate. However, in practice numerical solutions become prone to computational errors for large $2(m_1+m_2)$ and the method described for the transcendental eigenvalue problem are preferred. A fuller discussion of these numerical issues, solution methods and derivation of the eigenvalue problem in Eq. (25) can be found in Ref. [28].

3.3.2. Ratio of propagation constants irrational: transcendental eigenvalue problem

If μ_y/μ_x is irrational, then the algebraic eigenvalue problem (25) cannot be formed. Instead, the eigenvalue problem of Eq. (11), for given ω, can be written as

$$\overline{\mathbf{D}}(\lambda_x, \lambda_y)\mathbf{q}_1 = \mathbf{0} \tag{27}$$

where

$$\lambda_x = \mathrm{e}^{-\mathrm{i}kL_x\cos\,\theta}, \quad \lambda_y = \mathrm{e}^{-\mathrm{i}kL_y\sin\,\theta} \tag{28}$$

The problem thus reduces to finding the complex values of k for which

$$g(k) = \left|\overline{\mathbf{D}}(\lambda_x, \lambda_y)\right| = \mathbf{0} \tag{29}$$

It can be shown [28] that $g(k)$ is a holomorphic function whose real and imaginary parts satisfy Laplace's equation. It is continuous and continuously differentiable with respect to k and a range of methods exist for finding roots to Eq. (29). These include Newton's method, Newton's eigenvalue iteration method [33,34], Powell's method [35], the interval Newton method [36–38], by contour integration [39] and Muller's method

[40]. In the examples below and in Ref. [28] a variant of Powell's method implemented as the function *fsolve* in Matlab was used. If μ_y/μ_x is irrational there is in general an infinity of solutions, of which only a few are of interest, the remainder lying far from the origin in the complex k-plane.

3.4. Numerical issues

3.4.1. Finite element discretisation and dispersion errors

As with conventional FEA, FE discretisation errors become significant if the size of the element is too large [29]. As a rule-of-thumb, there should be at least 6 or so elements per wavelength. These errors also depend on the element aspect ratio and the direction of wave propagation. As in 1-dimensional WFE applications [41], if the size of the element is too small then care must be taken in numerical computations because round-off errors can occur if the dynamic stiffness matrix is to be calculated (i.e. if $\|\omega^2\overline{\mathbf{M}}\| \ll \|\overline{\mathbf{K}}\|$).

3.4.2. Spatial discretisation and periodic structure effects

In common with one-dimensional WFE applications, more significant issues arise because the original structure is continuous while the WFE model is a lumped, discrete, spring-mass structure which is spatially periodic with periods L_x and L_y in the x and y directions. For low frequencies, i.e. for wavelengths which are long compared to the size of the element, there are no significant consequences of this and the WFE model predicts the wavenumbers with good accuracy. However at higher frequencies, or for shorter wavelengths, there are substantial differences and periodic structure phenomena arise [42–45]. However, at such frequencies the accuracy of the FE description breaks down completely, so the issue is one of determining which solutions to the eigenvalue problem are artifacts of the spatial discretisation and which are valid estimates of wavenumbers in the continuous structure.

First, there is the issue of spatial discretisation and consequent aliasing effects. These arise because if, for a given frequency, if (μ_x, μ_y) is a solution to Eq. (11) for the propagation constants then so, too, is $(\mu_x+2m_x\pi, \mu_y+2m_y\pi)$ for any integral m_x, m_y, since they yield the same values for λ_x and λ_y. Thus the wave modes and frequencies are periodic functions of the propagation constants. This is a well-known effect for periodic structures [42]. In practical applications this is not important because the FE discretisation is known to be inaccurate for $\mu > \pi/3$ or thereabouts.

Secondly, periodic structures are known to exhibit a pass- and stop-band structure, in that disturbances can propagate freely only in certain frequency ranges, otherwise they decay with distance [42–44]. For a two-dimensional element with n dofs per node there will be n propagation surfaces. The bounds of these pass and stop bands are related to the natural frequencies of the periodic element under various boundary conditions [42–45].

It is worth noting that for elements with rigid body modes (i.e. those for which the stiffness matrix is singular), $\omega = 0$ is a cut-off frequency so that at least one wave must propagate from $\omega = 0$, and this wave must represent a wave in the continuous structure.

3.4.3. Sensitivity analysis and waves in the continuous structure

One issue might be to determine which numerical solutions for the discrete structure represent wave motion in the continuous structure and which are artifacts of the spatial discretisation. This can be achieved by determining the sensitivities of the estimated propagation frequencies or constants to the dimensions of the element, since the bounds of the pass and stop bands depend on the natural frequencies of the element with certain boundary conditions [42–45]. Thus increasing the size of the element both decreases the stiffness and increases the mass, hence reducing the bounding frequencies. Wavenumber estimates which are periodic artifacts are thus sensitive to the dimensions of the element whereas those which provide estimates of wavenumbers in the continuum are insensitive to such changes. The sensitivities can be found by simple re-meshing. Alternatively they can be evaluated analytically. For a given solution to Eq. (9), the derivative of the eigenvalue ω^2 with respect to a parameter L is [32]

$$\frac{\partial \omega_j^2}{\partial L} = \boldsymbol{\psi}_j \left[\frac{\partial \overline{\mathbf{K}}}{\partial L} - \omega_j^2 \frac{\partial \overline{\mathbf{M}}}{\partial L} \right] \boldsymbol{\phi}_j \tag{30}$$

The matrix derivatives or sensitivities are often available in commercial packages. If the consequent sensitivity

$$\frac{L}{\omega_j^2}\frac{\partial \omega_j^2}{\partial L} = O(1) \tag{31}$$

then the solution is a periodic artefact.

4. Numerical examples

In this section various numerical examples are presented to illustrate the application of the WFE method to plates. Further examples of orthotropic, thick and laminated plates and more detailed discussion can be found in Ref. [28].

4.1. Thin isotropic plate

Consider the flexural vibrations of a thin, isotropic plate lying in the x,y plane. The wavenumbers are such that [1,2]

$$\sqrt{k_x^2 + k_y^2} = \pm k_f, \pm \mathrm{i}k_f \tag{32}$$

where

$$k_f = \sqrt[4]{\frac{\rho h \omega^2}{D}} \tag{33}$$

is the flexural wavenumber and where ρ, h and D are the density, thickness and bending stiffness, respectively. To illustrate the WFE approach a square, 4-noded element of side $L_x = L_y = L$ is taken, with 3 dofs at each node, transverse displacement and the two rotations θ_x and θ_y. The shape function is a complete cubic with two quartic terms, x^3y and xy^3. The element mass and stiffness matrices are well-known (see e.g. Ref. [29], but note typographical errors). The non-dimensional parameters

$$\mu = \sqrt{\Omega}; \quad \mu = kL, \quad \Omega = \omega L^2\sqrt{\frac{\rho h}{D}} \tag{34}$$

are introduced.

The dispersion curves for real μ, i.e. for free wave propagation, are shown in Fig. 3 for $\theta = 0$. They are found by the eigensolution of Eq. (9), which has 3 solutions for Ω^2 for given μ. The WFE solutions are periodic functions of μ with period 2π because of the spatial periodicity. There are 3 pass bands whose cut-off frequencies, 0 and $\Omega_{a,b,c,d}$, are indicated in the Figure. Also shown is the analytical solution for the continuous plate. The first pass band ($\Omega < \Omega_a$) of the WFE results gives accurate results for μ up to $\pi/3$ or so. Fig. 4 shows the three solutions for μ as a function of Ω. The first is real in the pass bands and becomes complex in the stop bands. The other two are imaginary, with one accurately representing the evanescent waves while the other is a result of the FE discretisation. The first two eigenvalues are inaccurate for $\mu > \pi/3$ or so due to discretisation errors and break down completely for $\mu > \pi$ because of periodic structure phenomena. The wave mode shapes (i.e. the right eigenvectors) for the first two solutions are more-or-less constant in the y-direction while the third shows a substantial change in shape (the displacements along the edge are positive at the nodes and negative between them).

Fig. 5 shows the relative error in the estimated frequency of propagation as a function of the direction of propagation and for elements of various aspect ratios. The frequency corresponds to 400 Hz in a 0.5 mm thick steel plate. The element is square. The error increases as the size of the element increases and is also a maximum for propagation in the direction of the diagonal across the element. These results were found by solving the transcendental eigenvalue problem to which there are multiple solutions. As one example, the solutions in the region $-10 < \mathrm{Re}\{\mu\} < 10$ for the square element for waves propagating in the direction $\theta = \pi/3$ are shown in Fig. 6. The four analytical solutions are predicted accurately and there are numerous other solutions for which $|\mu|$ is large. The sensitivities with respect to the element length of the solutions which truly

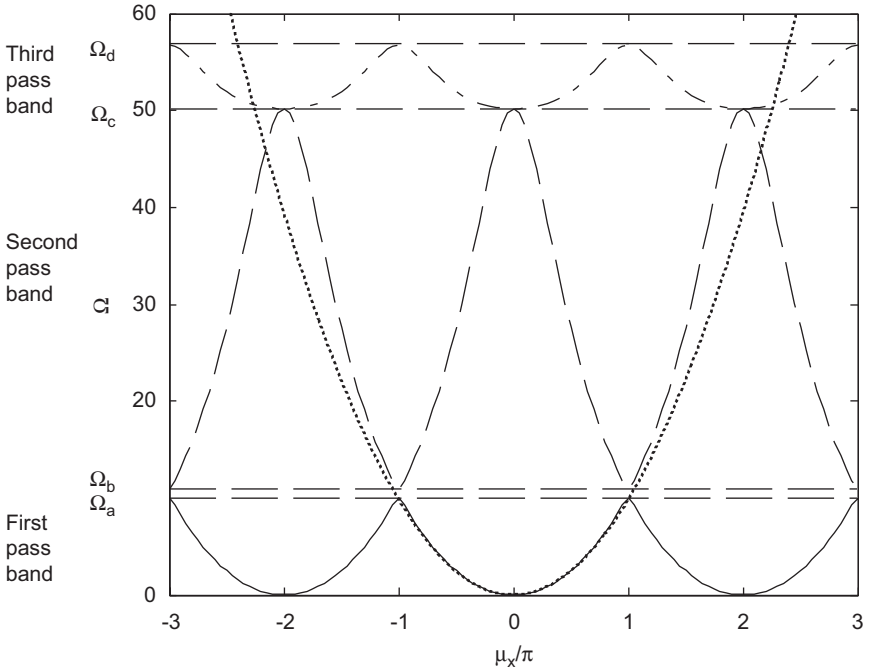

Fig. 3. Dispersion curves for isotropic plate, propagating waves, $\theta = 0$: …… analytic solution; WFE results: —— first, - - - second and - · - · third pass bands.

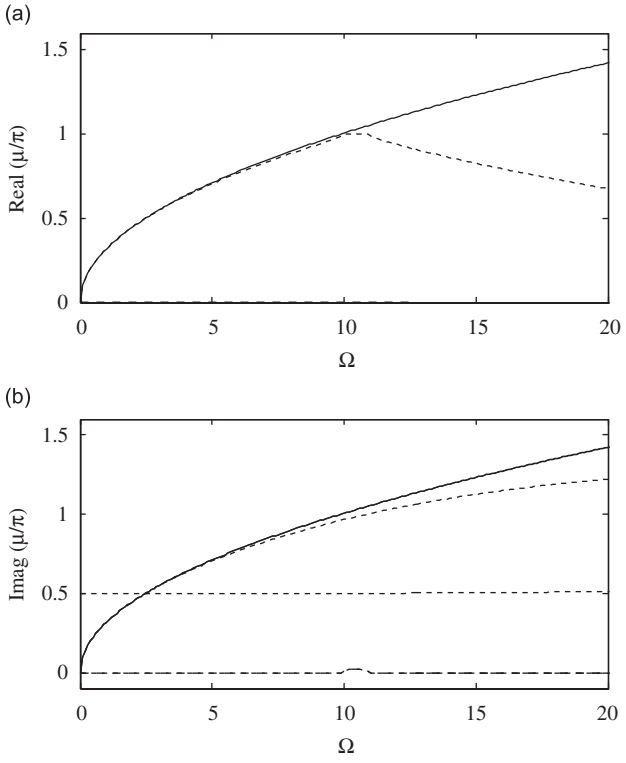

Fig. 4. Dispersion curves for isotropic plate, $\theta = 0$: —— analytic solution; - - - WFE results; (a) Re$\{\mu\}$, and (b) Im$\{\mu\}$.

represent motion in the continuum are insensitive to the element length while those that are artefacts of the spatial periodicity have sensitivities approximately equal to 1.

4.2. Thick isotropic plate

There are various plate theories, each of which involves various assumptions and approximations concerning the distribution of stresses, strains or displacements across the plate. The most common finite elements have 6 dofs per node and implement Mindlin-Reissner shell theory [1–3] in which shear deformation and rotary inertia are included. At higher frequencies this model becomes inaccurate. An alternative in FEA is to model the structure through the thickness using a number of solid elastic elements. Henceforth, 8-noded elements with 3 displacement dofs per node are used in the numerical simulations. These were implemented as SOLID45 elements in ANSYS.

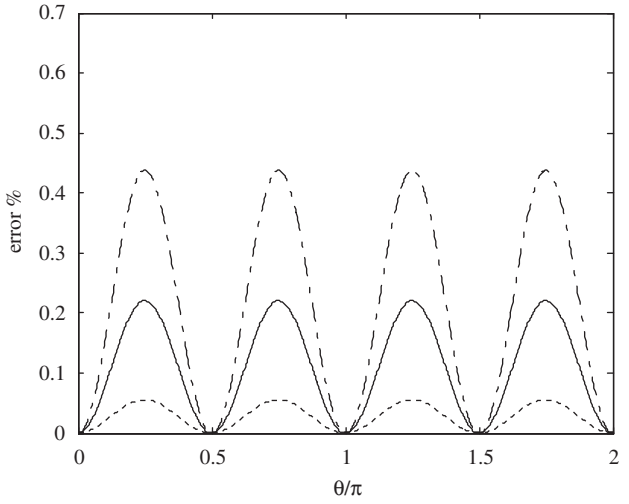

Fig. 5. Relative error in estimated frequency as a function of θ for propagating waves in an isotropic plate, $\Omega = 0.0837$, $\mu = 0.289$: ____ $L_y/L_x = 1$; …… $L_y/L_x = 1/2$; - · - · - $L_y/L_x = \sqrt{2}$.

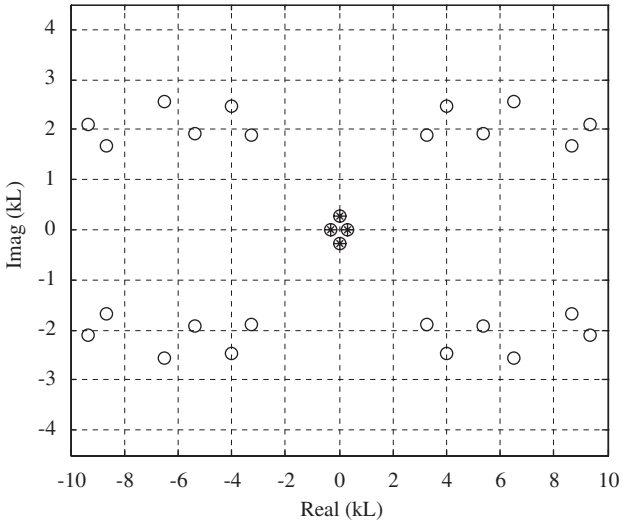

Fig. 6. Free wave propagation in an isotropic plate in direction $\theta = \pi/3$, $\Omega = 0.0837$, $\mu = 0.289$: + analytical solutions; ○ numerical solutions to the transcendental eigenvalue problem.

In this section an aluminium plate ($E = 7.1 \times 10^{10}\,\mathrm{N\,m^{-2}}$; $\rho = 2.7 \times 10^{3}\,\mathrm{kg\,m^{-3}}$; $\nu = 0.329$) of thickness $h = 15\,\mathrm{mm}$ is considered. It was meshed using 50 solid elements with $L_x = L_y = 1\,\mathrm{mm}$, although fewer elements provide accurate results in the frequency range considered. Results are presented in terms of the dimensionless frequency

$$\Omega = \frac{h\omega}{\pi c_T}; \quad c_T = \sqrt{\frac{E}{2\rho(1+\nu)}} \tag{35}$$

Dispersion curves are shown in Fig. 7, with there being real, imaginary and complex conjugate solutions. Only those solutions which propagate for $\Omega < 2.5$ are shown. There are 3 propagating waves for $\Omega < 1$—these correspond to primarily flexural, shear and extensional waves. Higher order modes across the thickness cut on at $\Omega = 1$, these being primarily anti-symmetric shear and extensional waves. A pair of complex conjugate wavenumbers bifurcates into a pair of propagating waves with real wavenumbers around $\Omega \approx 1.8$. One of these propagating waves has phase and group velocities of opposite sign. The wave mode shapes are discussed in Ref. [28].

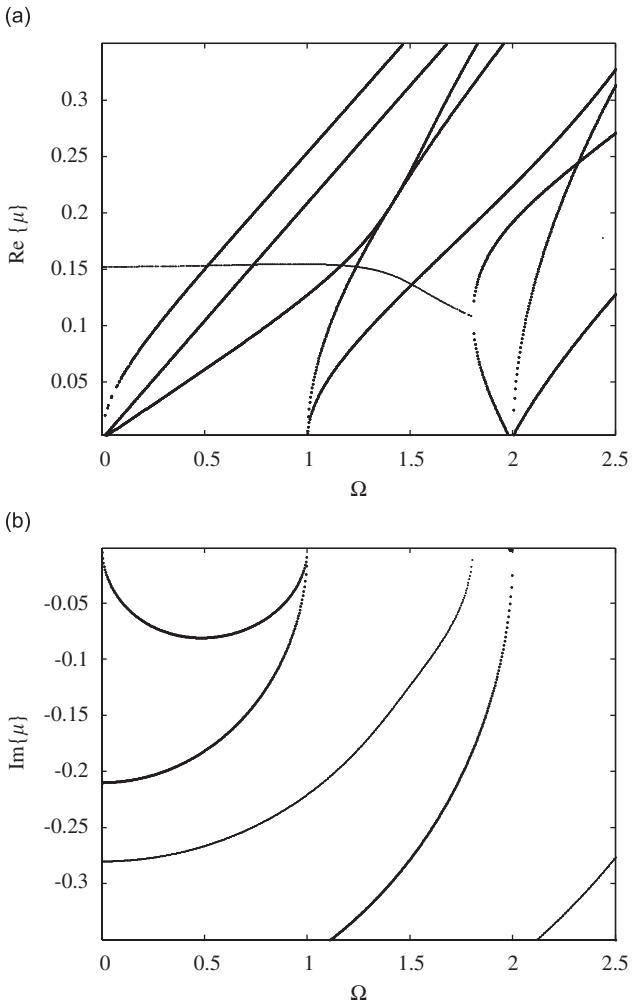

Fig. 7. Dispersion curves for a thick isotropic plate, $\theta = 0$: (a) real and (b) imaginary parts; …… pure real and pure imaginary wavenumbers; …… complex wavenumbers.

4.3. Asymmetric laminated plate

Consider a laminated plate comprising two 5 mm thick layers of GFRP with asymmetric ply-stacking of [0/90]. Such a structure was considered by Chackraborty and Gopalakrishnan [46] using a spectral finite element and dynamic stiffness approach. Material and geometric properties are taken from [46]. Fig. 8 shows the real-valued dispersion curves for k_x when $k_y = 50\,\mathrm{m}^{-1}$ together with the results using the method in Ref. [46]. The WFE model involved two elements across the cross-section. The agreement is good at low frequencies and less good as frequency increases. This is due at least in part to the fact that Chackraborty and Gopalakrishnan used a first-order layer-wise laminate theory which becomes less accurate as frequency increases.

The WFE approach can be applied equally to laminates of arbitrary complexity, with an arbitrary number of layers. One further advantage of the WFE approach is that the dispersion curves can be readily evaluated for different directions of propagation. As an example, Fig. 9 shows the real-valued dispersion curves for various values of θ.

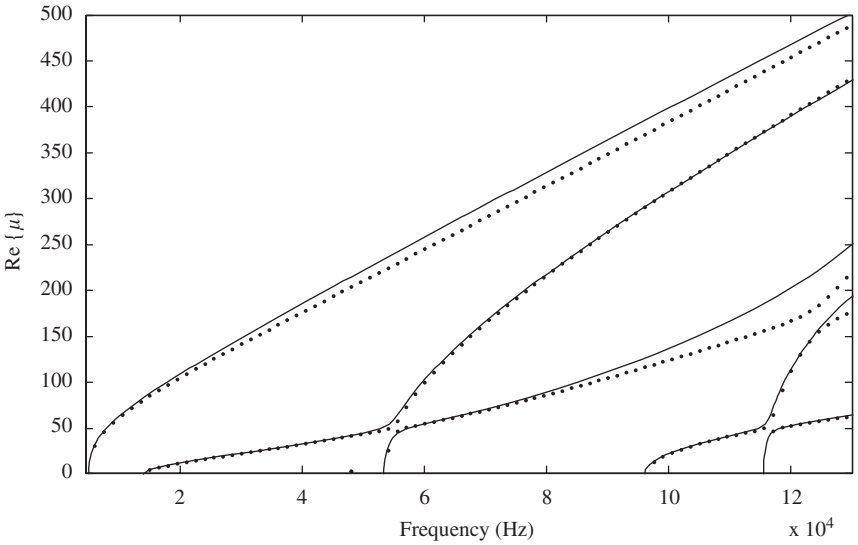

Fig. 8. Asymmetric cross-ply laminate: real-valued dispersion curves, $k_y = 50\,\mathrm{m}^{-1}$: —— WFE results and …… theory of [43].

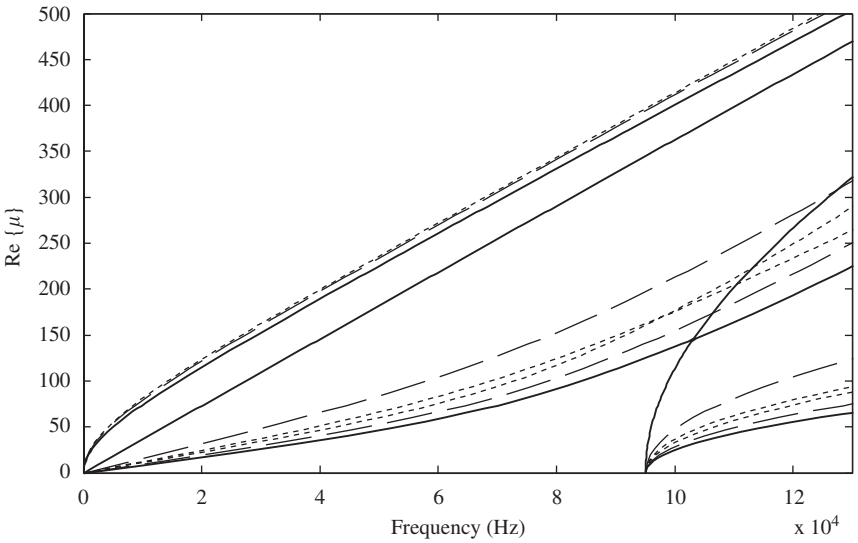

Fig. 9. Asymmetric cross-ply laminate: real-valued dispersion curves: —— $\theta = 0°$, …… $\theta = 45°$ and - · - · $\theta = 60°$.

4.4. Anti-symmetric cross-ply sandwich panel

The final example is an asymmetric, cross-ply laminated sandwich panel. The two outer skins comprise 4 orthotropic sheets of 0.5 mm thick glass-epoxy. The stacking sequences of the top and bottom skins are [0/45/45/0] and [45/0/0/45], respectively. The core is 10 mm thick Rohacell foam ($\rho = 1100\,\mathrm{kg}^{-3}$, $E = 0.18 \times 10^9\,\mathrm{Nm}^{-2}$, $v = 0.286$). The material properties of each glass-epoxy sheet are: $E_x = E_y = 5.4 \times 10^{10}$, $E_z = 4.8 \times 10^9$; $G_{xz} = G_{yz} = 1.78 \times 109$, $G_{xy} = 3.16 \times 10^9$; $v_{xz} = 0.06$; $\rho = 2000$, all in S.I. units. To model the structure 4 SOLID45 elements with $L_x = L_y = 1$ mm were used for each skin and 10 elements used for the core.

Fig. 10 shows the dispersion curves for waves propagating in the direction $\theta = 0$. Complicated behaviour is again observed, with propagating waves cutting off with non-zero (real) wavenumber and there being branches for which the phase and group velocities are of opposite sign.

The eigenvectors indicate the deformations under the passage of a wave, while the time average kinetic and potential energies follow from the mass and stiffness matrices and the power associated with the individual dofs follows from the nodal displacements and forces. These reveal the characteristics of the wave mode. For example, Fig. 11 shows the deformations of the cross-section for the three propagating wave branches at 2 kHz. (These figures are not drawn to scale—for example in Fig. 11(a) the displacements in the x direction have been magnified relative to those in the z-direction so that bending deformation in the skins can be more

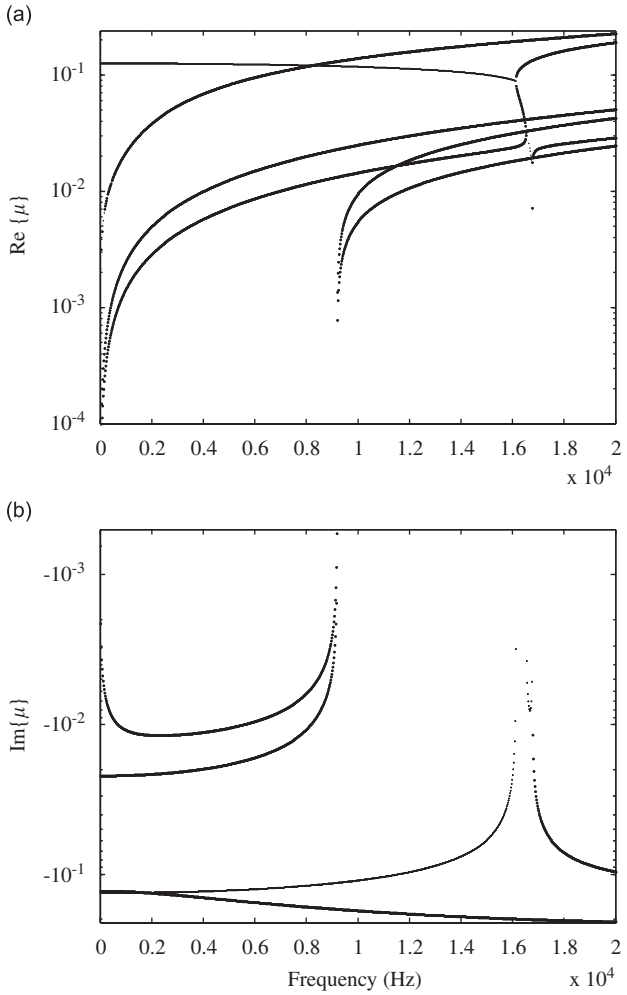

Fig. 10. Asymmetric cross-ply laminate sandwich panel, dispersion curves for $\theta = 0$: (a) real and (b) imaginary parts; …… pure real and pure imaginary wavenumbers; …… complex wavenumbers.

clearly observed.) Branch 1, i.e. that with the largest wavenumber (Fig. 11(a)) predominantly involves bending of the skins with some shear in the core. The displacements in the y-direction are negligible, in the z-direction are almost constant across the cross-section and in the x direction arise from shear and rotation of the laminas. Branch 2 (Fig. 11(b)) is a shear wave, involving displacements primarily in the y-direction, while the wave of branch 3 (Fig. 11(c)) is an axial wave, so that the displacements are primarily in the x direction, although some Poisson contraction in the z direction can be observed.

These three low-frequency branches correspond more or less to familiar plate waves. At higher frequencies, however, the behaviour becomes much more complicated. For example, Fig. 12 shows the deformation under the passage of the waves in the 4th and 5th propagating branches at 10 kHz. Branch 4 (Fig. 12(a)) is the first anti-symmetric shear mode, involving counterphase shear motion in the two skins and shear in the core. Displacements in the x and z directions are small. Branch 5 (Fig. 12(b)) involves counterphase anti-symmetric extensional motion in the skins, again with shear in the core. At higher frequencies still the motion is complicated and the effects of the asymmetric construction become noticeable. For example, at 17.5 kHz the propagating branch with the second largest wavenumber involves axial motion of the core (Fig. 12(c)), together with Poisson contraction in the z-direction. There is also noticeable shear motion in the y-direction.

5. Concluding remarks

In this paper a wave/finite element (WFE) method for the analysis of wave motion in two-dimensional structures was described. The structures are homogeneous in two dimensions but the properties might vary through the thickness. The method involves post-processing the mass and stiffness matrices of a segment of the structure, produced using conventional FE methods. The size of the FE model is very small. Emphasis was placed on a 4-noded, rectangular segment, although other element types can be used. Periodicity conditions

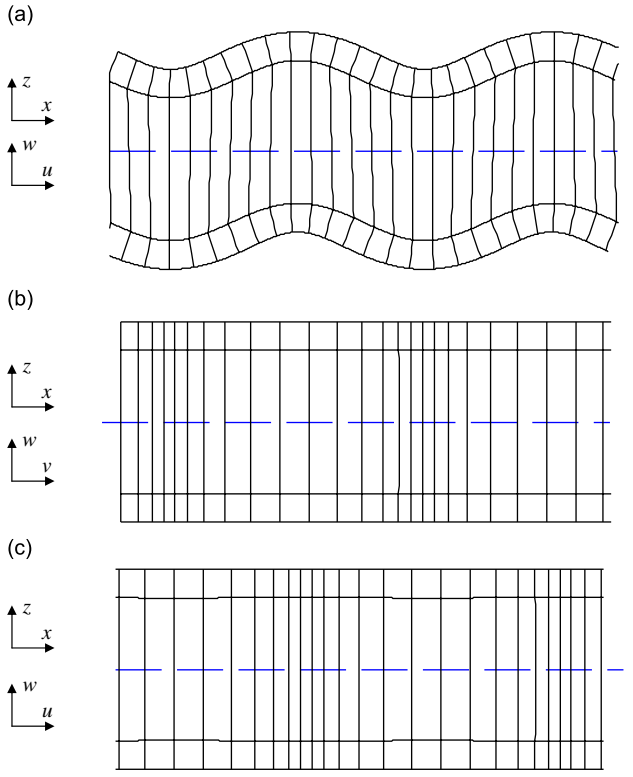

Fig. 11. Wave modes at 2 kHz (not to scale): (a) branch 1, displacements u and w in x and z directions; (b) branch 2, displacements v and w in y and z directions; (c) branch 3, displacements u and w in x and z directions. The top and bottom surfaces of the skins and core and the motion of various cross-sections are shown as functions of the distance x along the laminate at one instant of time.

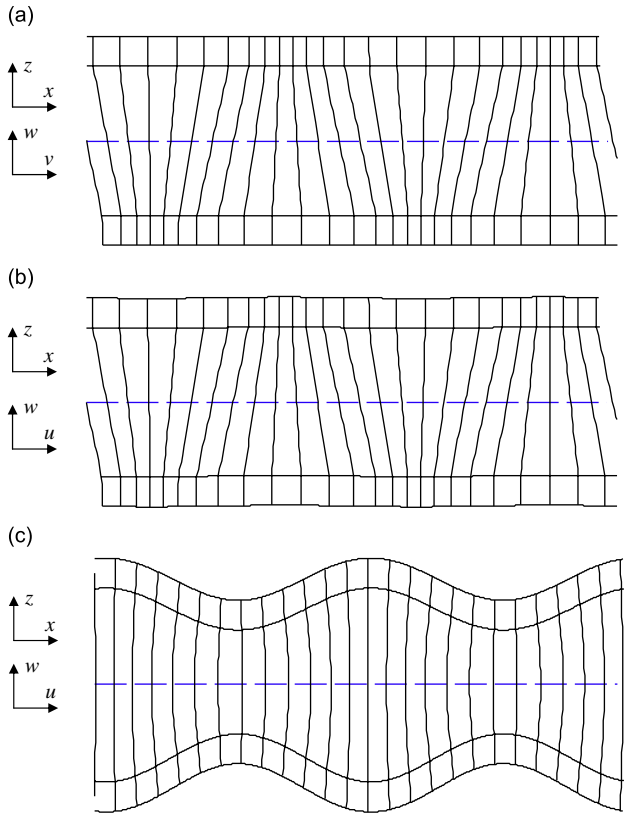

Fig. 12. Wave modes (not to scale): (a) branch 4 at 10 kHz, displacements v and w in y and z directions; (b) branch 5 at 10 kHz, displacements u and w in x and z directions; (c) branch with 2nd largest wavenumber at 17.5 kHz, displacements u and w in x and z directions. The top and bottom surfaces of the skins and core and the motion of various cross-sections are shown as functions of the distance x along the laminate at one instant of time.

were then applied using the approach developed by Abdel-Rahman [7] in the context of FE analysis of periodic structures. Eigenproblems of various forms then arise, the form depending on the nature of the problem at hand. These might be linear, quadratic, polynomial or transcendental eigenproblems. The solutions sought might be real-valued wavenumbers for propagating waves in an undamped structure, waves with real, imaginary or complex wavenumbers and a given trace wavenumber in one direction, or waves of all types propagating in a given direction. Numerical issues were discussed: the segment must be small enough to avoid significant finite element discretisation errors and some solutions for the discretised structure are artefacts of the spatial periodicity rather than being representative of wave motion in the continuum. Which of these is the case can be readily determined by re-meshing or by sensitivity analysis.

Examples of thin and thick plates and various laminates were given. In the last two examples considered, developing an analytical model is a formidable task which inevitably involves assumptions and approximations. Even then, only a numerical solution to the dispersion equation is possible. The WFE approach, however, merely involves the systematic post-processing of element matrices typically found using a commercial FE package, in this case ANSYS. This is one of the main strengths of the WFE approach, in that the meshing capabilities and the wealth of existing element libraries can be exploited. Accurate predictions of the dispersion relations can be found at negligible computational cost.

Acknowledgements

Part of this work was carried out while the first author was an Erskine Visiting Fellow at the University of Canterbury, New Zealand. Part of this work was carried out while the second author held a Fellowship funded

by the European Doctorate in Sound and Vibration Studies. The authors are grateful for the support provided.

References

[1] K.F. Graff, *Wave Motion in Elastic Solids*, Dover Publications Inc., New York, 1975.
[2] L. Cremer, M. Heckl, B.A.T. Petersson, *Structure-Borne Sound*, third ed., Springer, Berlin, 2005.
[3] R.D. Mindlin, Influence of rotatory inertia and shear on flexural motions of isotropic, elastic plates, *Journal of Applied Mechanics* 18 (1951) 31.
[4] H. Lamb, On waves in an elastic plate, *Proceedings of the Royal Society of London* A93 (1917) 114.
[5] J.N. Reddy, *Mechanics of Laminated Composite Plates: Theory and Analysis*, CRC Press, Boca Raton, FL, 1996.
[6] D.J. Mead, *Passive Vibration Control*, Wiley, New York, 2000.
[7] Y.A. Abdel-Rahman, Matrix Analysis of Wave Propagation in Periodic System, Ph.D. Thesis, University of Southampton, 1979.
[8] B.R. Mace, D. Duhamel, M.J. Brennan, L. Hinke, Finite element prediction of wave motion in structural waveguides, *Journal of the Acoustical Society of America* 117 (2005) 2835–2843.
[9] D. Duhamel, B.R. Mace, M.J. Brennan, Finite element analysis of the vibration of waveguides and periodic structures, *Journal of Sound and Vibration* 294 (2006) 205–220.
[10] D.J. Thompson, Wheel-rail noise generation, part III: rail vibration, *Journal of Sound and Vibration* 161 (1993) 421–446.
[11] L. Gry, C. Gontier, Dynamic modelling of railway track: a periodic model on a generalized beam formulation, *Journal of Sound and Vibration* 199 (1997) 531–558.
[12] L. Houillon, M.N. Ichchou, L. Jezequel, Wave motion in thin-walled structures, *Journal of Sound and Vibration* 281 (2005) 483–507.
[13] M. Maess, N. Wagner, L. Gaul, Dispersion curves of fluid filled elastic pipes by standard FE models and eigenpath analysis, *Journal of Sound and Vibration* 296 (2006) 264–276.
[14] J.M. Mencik, M.N. Ichchou, Wave finite elements in guided elastodynamics with internal fluid, *International Journal of Solids and Structures* 44 (2007) 2148–2167.
[15] J.M. Mencik, M.N. Ichchou, Multi-mode propagation and diffusion in structures through finite elements, *European Journal of Mechanics, A—Solids* 24 (5) (2005) 877–898.
[16] R.M. Orris, M. Petyt, A finite element study of harmonic wave propagation in periodic structures, *Journal of Sound and Vibration* 33 (2) (1974) 223–236.
[17] R.M. Orris, M. Petyt, Random response of periodic structures by a finite element technique, *Journal of Sound and Vibration* 43 (1) (1975) 1–8.
[18] D.J. Mead, Wave propagation in continuous periodic structures: research contributions from Southampton, 1964–1995, *Journal of Sound and Vibration* 190 (3) (1996) 495–524.
[19] J. Signorelli, A.H. Von Flotow, Wave propagation, power flow and resonance in a truss beam, *Journal of Sound and Vibration* 126 (1) (1988) 127–144.
[20] M.L. Accorsi, M.S. Bennett, A finite element based method for the analysis of free wave propagation in stiffened cylinders, *Journal of Sound and Vibration* 148 (2) (1991) 279–292.
[21] M.S. Bennett, M.L. Accorsi, Free wave propagation in periodically ring-stiffened shells, *Journal of Sound and Vibration* 171 (1) (1994) 49–66.
[22] L. Gavric, Computation of propagative waves in free rail using a finite element technique, *Journal of Sound and Vibration* 184 (1995) 531–543.
[23] S. Finnveden, Spectral finite element analysis of the vibration of straight fluid-filled pipes with flanges, *Journal of Sound and Vibration* 199 (1996) 125–154.
[24] P.J. Shorter, Wave propagation and damping in linear viscoelastic laminates, *Journal of the Acoustical Society of America* 115 (2004) 1917–1925.
[25] M. Ruzzene, F. Scarpa, F. Soranna, Wave beaming effects in two-dimensional cellular structures, *Smart Materials and Structures* 12 (2003) 363–372.
[26] D. Duhamel, Finite element computation of Green's functions, *Engineering Analysis with Boundary Elements* 31 (2007) 919–930.
[27] J.F. Doyle, *Wave Propagation in Structures: Spectral Analysis using Fast Discrete Fourier Transforms*, second ed., Springer, Berlin, 1997.
[28] E. Manconi, The Wave Finite Element Method for 2-dimensional Structures, Ph.D. Thesis, University of Parma, 2008.
[29] M. Petyt, *Introduction to Finite Element Vibration Analysis*, Cambridge University Press, New York, USA, 1990.
[30] E. Manconi, B.R. Mace, Modelling wave propagation in two-dimensional structures using a wave/finite element technique. ISVR Technical Memorandum No. 966, 2007.
[31] R.S. Langley, Wave motion and energy flow in cylindrical shells, *Journal of Sound and Vibration* 169 (1994) 29–42.
[32] S. Adhikari, M.I. Friswell, Eigenderivative analysis of asymmetric non-conservative systems, *International Journal for Numerical Methods in Engineering* 51 (2001) 709–733.
[33] K.V. Singh, Y.M. Ram, Transcendental eigenvalue problem and its applications, *AIAA Journal* 40 (2002) 1402–1407.
[34] W.H. Yang, A method for eigenvalues of sparse λ-matrices, *International Journal for Numerical Methods in Engineering* 19 (1983) 943–948.

[35] M.J.D. Powell, A Fortran subroutine for solving systems of nonlinear algebraic equations, in: P. Rabinowitz (Ed.), *Numerical Methods for Nonlinear Algebraic Equations*, 1970 (Chapter 7).
[36] L.E. Bateson, M.A. Kelamanson, C. Knudsen, Solution of a transcendental eigenvalue problem via interval analysis, *Computers and Mathematics with Applications* 38 (1999) 133–142.
[37] R.E. Moore, *Interval Analysis*, Prentice-Hall, Englewood Cliff, NJ, 1966.
[38] E. Hansen, *Global Optimization using Interval Analysis*, Pure and Applied Mathematics, USA, 1992.
[39] E. Kreyszig, *Advanced Engineering Mathematics*, Wiley, New York, 1999.
[40] C.F. Gerald, *Applied Numerical Analysis*, Addison-Wesley, Reading, MA, 1999.
[41] Y. Waki, B.R. Mace, M.J. Brennan, Waveguide finite element modelling: numerical issues and application to simple waveguides, *Proceedings of ISMA 2006*, Leuven, 2006.
[42] L. Brillouin, *Wave propagation in periodic structures*, Dover Publications, New York, 1953.
[43] D.J. Mead, Wave propagation and natural modes in periodic system: I. Mono-coupled systems, *Journal of Sound and Vibration* 40 (1975) 1–18.
[44] D.J. Mead, Wave propagation and natural modes in periodic systems: II. Multi-coupled systems, with and without damping, *Journal of Sound and Vibration* 40 (1975) 19–39.
[45] D.J. Mead, S. Parthan, Free wave propagation in two-dimensional periodic plates, *Journal of Sound and Vibration* 64 (1979) 325–348.
[46] A. Chackraborty, S. Gopalakrishnan, A spectrally formulated finite element for wave propagation analysis in layered composite media, *Journal of Solid and Structures* 41 (2004) 5155–5183.